



Assessment of responses of North Atlantic winter SST to the NAO in 13 CMIP5 models on the interannual scale

Yujie Jing^{1,2}, Yangchun Li^{1,2}, Yongfu Xu^{1,2}

¹State Key Laboratory of Atmospheric Boundary Layer Physics and Atmospheric Chemistry, Institute of Atmospheric Physics, Chinese Academy of Sciences, Beijing 100029, China

²Department of Atmospheric Chemistry and Environmental Sciences, College of Earth and Planetary Sciences, University of Chinese Academy of Sciences, Beijing 100049, China

Correspondence: Yangchun Li (lych@mail.iap.ac.cn)

10

Abstract. This study evaluates the response of winter-averaged sea surface temperature (SST) to the winter North Atlantic Oscillation (NAO) simulated by 13 CMIP5 Earth System Models in the North Atlantic (NA) (0-65°N) on the interannual scale. Only 7 models can reproduce an observed tripolar pattern of the response of SST anomalies to the NAO, and most of the models cannot generate the observed impact of variations of the turbulent heat flux on the response of SST anomalies to the NAO. In the subpolar NA (45-65°N) where the influences of sensible / latent heat fluxes on SST are obvious, most of the models simulate a positive response of SST to the turbulent heat flux in the large area of this region, which is opposite to the observations, and probably generate the incorrect positive response of SST to the NAO in some models. In the subtropical NA (25-45°N), the observations show a significant influence of

15



latent heat flux (LHF) on SST, but the overestimated oceanic role in the interaction of the LHF and SST in most
20 CMIP5 models results in an incorrect positive response of SST anomalies to the LHF anomalies in a large area of the
subtropical NA. Besides the turbulent heat flux, the meridional advection is also important to the change of the SST in
the NA. The analysis of the simulated and observed results shows that NAO-driven meridional advection can cause the
increase / decrease of SST during the positive phase of the NAO in the subtropical / subpolar NA. This is probably one
of the main causes why the models can simulate the realistic positive response of SST anomalies to the NAO in the
25 subtropical NA, but the strength of the positive response is relatively weak.

Keywords: NAO; SST; turbulent heat flux; meridional advection; interannual scale

1. Introduction

The most notable climatic event in the North Atlantic (NA) is a strong inverse relationship between Iceland's and
the Azores' monthly mean sea level pressure (most significant in winter), which is called the North Atlantic Oscillation
30 (NAO) (Walker, 1924). Studies have shown that the NAO has a significant impact on climate change in the Northern
Hemisphere, including the significant impact on temperature and precipitation in Europe and the NA (Trigo et al.,
2002). Because of the internal atmospheric dynamic process, the NAO is closely related to the location and intensity of
storm track in the NA (Rivière and Orlanski, 2007). In addition, the NAO not only impacts the atmospheric field, but
also the oceanic field through air-sea interactions, such as the sea surface temperature (SST) in the NA.

35 The influence of the atmospheric anomalies on SST is mainly reflected in the change of sea surface heat flux



driven by the change of local wind stress in the NA (Chen et al., 2015; Han et al., 2016), and this mechanism mainly occurs on the interannual scale (Eden and Jung, 2001). The NAO is the most active climatic event in the Atlantic-Europe region in winter. Many studies have pointed out that the tripolar pattern of SST anomalies is driven by turbulent heat flux anomalies (sensible and latent heat fluxes, SHF and LHF) associated with the NAO (Cayan, 1992; Marshall and Gareth, 2003; Visbeck et al., 2003; Deser et al., 2010). Specifically, during the positive period of the NAO, the ocean loses energy in the subpolar and tropical NA due to the strengthening of the westerly winds and the northeast trade winds, respectively; while in the mid-latitude NA, the wind speed is weakened due to the easterly anomalies superimposed on a background of mean westerlies, which weakens the turbulent heat flux from ocean to the atmosphere, and the warm air advection caused by the southerly winds on the east coast of the United States makes the oceans gain energy from the atmosphere. Therefore, during the positive period of the NAO, the SST in the subtropical NA increases (Zhou et al., 2006; Deser et al., 2010). Other studies suggest that during the positive period of the NAO, the Atlantic meridional overturning circulation (AMOC) is intensified, leading to uniform SST warming (Sun et al., 2015), which probably occurs on the interdecadal and multidecadal scales (Gastineau et al., 2012). In addition, SST anomalies also have feedback on the atmosphere, and the dominant heat flux forcing to the NAO is associated with the later summer horseshoe SST forcing (Wen et al., 2005). Furthermore, temperature anomalies of deeper seawater can also generate heat flux forcing to the atmosphere on long timescales (Yulaeva et al., 2001; Sutton and Mathieu, 2002).

Due to the time and space limitations of observations, many models are used to study the NAO. For example, Stoner et al. (2009) have evaluated the winter NAO simulated by coupled atmosphere-ocean general circulation



models (AOGCMs), and pointed out that the spatial pattern of the NAO is more reasonable, but the action center of
55 high pressure is west of the observation comparing with observation. In addition, Woollings. (2014) have simulated the
mechanism of change of the NAO with an atmospheric circulation model (HiGEM), and proposed the impact of jets in
the upper troposphere on the change of the NAO. The Coupled Model Intercomparison Project Phase 5 (CMIP5)
(Taylor et al., 2012) includes more Earth system models with higher spatial resolution, which helps to better
understand ocean and atmospheric variability and their interaction. In recent years, more and more people have
60 realized that the evaluation of the CMIP5 Earth System Models (CMIP5-ESMs) is the basis for study by these models.
For example, Wang et al. (2017) paid attention to the ability of the CMIP5-ESMs to simulate annual NAO and found
that basically all models can reasonably reproduce the spatial distribution of the NAO. Meanwhile, Wang et al. (2014)
evaluated the global SST simulated by the CMIP5-ESMs and found that the SST in the Northern Hemisphere,
especially in the NA, is underestimated, and pointed out that it is mainly caused by the unreasonable simulation of
65 AMOC. Liu et al. (2013) evaluated the SST variability in the NA warm pool simulated by 19 CMIP5-ESMs, and
considered that the deviation of radiation balance caused by the CMIP5-ESMs' unreasonable simulation of high-level
cloud fraction can impact the SST variability. The relationship between the SST and NAO in the North Atlantic from
the CMIP5-ESMs has not been systematically evaluated, but it is of great significance to study the North Atlantic
variability and climate change in the entire Northern Hemisphere. Multiple observation-based studies have indicated
70 that there is a close connection and strong interaction between the NAO and the tripolar pattern of winter SST
anomalies (Czaja and Frankignoul., 2002; Chen et al., 2015). Therefore, the purpose of this paper is to evaluate



whether the CMIP5-ESMs can simulate the relationship between the NAO and SST in winter in the NA (0-65°N), to investigate the mechanism of the response of SST to the NAO, and to explore the deviation of models in simulating the response mechanism of SST to the NAO.

75 2. Data and methods

2.1 Data

The observation-based data in this study are monthly sea level pressure (SLP) from 1901 to 2010 from the reanalysis dataset of the 10-member ensemble of coupled climate reanalysis of the 20th century (CERA-20C) of the European Centre for Medium-Range Weather Forecasts (ECMWF) (apps.ecmwf.int/datasets/data/cera20c/levtype=sfc/type=an/), and the monthly SST data from 1870 to 2016, which was produced by the Hadley Centre Global Sea Ice and Sea Surface Temperature (HadISST, climatedataguide.ucar.edu/climate-data/sst-data-hadisst-v11, Rayner et al., 2003). The 10-m wind speed (vm10) data from 1836 to 2015 used here are based on a synthesis of NOAA-CIRES-DOE Twentieth Century Reanalysis (V3) monthly average meridional and zonal wind from 1948 to 2018 (https://www.esrl.noaa.gov/psd/data/gridded/data.20thC_ReanV3.monolevel.html, Compo et al., 2011). The monthly latent/sensible heat flux data from 1870 to 2016 used here are produced by NOAA-CIRES 20th Century Reanalysis version 2 (https://www.esrl.noaa.gov/psd/data/gridded/data.20thC_ReanV2.html, Compo et al., 2011). The sea water Y velocity data from 1981 to 2017, which was produced by the Global Ocean Data Assimilation System (GODAS,



https://www.esrl.noaa.gov/psd/data/gridded/data.godas.html, Behringer and Xue, 2004). The 13 Earth System Models
90 used for this work are from the historical experiment of CMIP5 (Table 1, cera-www.dkrz.de, Taylor et al., 2012). The
simulation results from these models provide the monthly average data of SLP, SST, latent/sensible heat net flux, and
sea water Y velocity during 1850–2005. In order to make comparisons and analyses between the simulated and
observed results, all variables are interpolated into a spatial resolution $1^\circ \times 1^\circ$ by linear interpolation, and the time range
of all variables from observations and models is 1902–2010 and 1897–2005, respectively.

95 2.2 Methods

Two definitions of the observation-based winter NAO are used in this work. The index proposed by Gong and
Wang (2000) is expressed as

$$I_{\text{NAO}} = P^*(35^\circ\text{N}, 10^\circ\text{W} \sim 10^\circ\text{E}) - P^*(65^\circ\text{N}, 10^\circ \sim 30^\circ\text{W}) \quad (1)$$

where P^* represents the normalized SLP. A three-point (10°W , 0°E , and 10°E for the high-pressure area and 10°W ,
100 20°W , and 30°W for the low-pressure area) spatial arithmetic average of P^* differences between the high- and
low-pressure area is used. The other NAO index is a site-based one from the Climate Analysis Section of the National
Center for Atmospheric Research (NCAR;
www.climatedataguide.ucar.edu/climate-data/hurrell-north-atlantic-oscillation-nao-index-station-based, Hurrell and
Deser, 2009).

105 Because the locations of the NAO action centers are different between the model and the observation, and



110

between the different models, we use the method proposed by Wang et al. (2017) and Zheng et al. (2013) to define the NAO index based on the results of the models. This method is basically similar to the one proposed by Gong and Wang (2000), in which the winter NAO index is defined as the difference in the normalized SLP, zonally averaged over the North Atlantic sector (30-80°N; 80°W–30°E), between the two latitudes that have the strongest negative correlation in SLP variability.

115

The winter duration used to define the winter NAO index / SST / wind speed / turbulent heat flux is December-January-February (DJF). For the variables of DJF, the January in the given year is used as the reference to obtain the winter variables. In other words, the variables for DJF of 1980 are obtained based on data in December of 1979 and January and February of 1980. For the winter variables, when calculating the seasonal average NAO index (DJF), the winter season average of SLP is firstly calculated, and then the NAO index is obtained.

Because the main cycles characterized by the interannual and decadal signs of the NAO are within 2-6 years and above 8 years, respectively (Jing et al., 2019), the interannual scale is extracted using a 2-6 year Lanczos band-pass filter. For the regression analysis between the NAO and ocean physical variables, the effective degree of freedom (DOF) is calculated following Bretherton et al. (1999):

120

$$\text{DOF} = N(1-r_1r_2)(1+r_1r_2) \quad (2)$$

Where N is the sample size, r1 and r2 are the lag-one autocorrelations of the two time series, respectively.

In order to understand the mechanisms of the impact of the NAO on SST, we need to know the main factors leading to the change of SST. The variability of SST is described by:



$$C_0 \frac{\partial SST'}{\partial t} = Q' + A' = Q_R' + Q_B' + A' \quad (3)$$

125
$$Q_B = -Q_S - Q_L \quad (4)$$

Here, C_0 is the thermal capacity of the upper mixed layer of the ocean, which is approximately constant, A is the divergence of ocean heat transport, Q is the air–sea heat flux and has both radiative (Q_R) and turbulent (Q_B) components. The turbulent heat fluxes are the sensible (Q_S , SHF) and latent (Q_L , LHF) heat fluxes (the positive value indicates the flux from the sea surface to the atmosphere). Among them, the sensible and latent heat fluxes are mainly related to wind speed (U) and SST, which are usually calculated by the following equations:

130

$$Q_S = \rho C_p C_S (SST - T_a) |\Delta \vec{U}| \quad (5)$$

$$Q_L = \rho L_p C_L (q_s - q_a) |\Delta \vec{U}| \quad (6)$$

where ρ is a near surface air density, C_p is the specific heat of the air, L_p is the latent heat of evaporation, C_S and C_L are the transfer coefficients of sensible and latent heat fluxes, respectively, T_a is the temperature of the atmosphere near the sea surface, $\Delta \vec{U} = \vec{U}_a - \vec{U}_s$ is the vector difference between the wind speed at the sea surface and the sea surface current speed, in which the current speed is often neglected, q_a and q_s correspond to saturation specific humidity of air over sea surface and sea surface temperature, respectively. q_s is usually calculated by the saturation humidit q_{sat} , for pure water at SST:

135

$$q_s = 0.98 q_{sat}(SST) \quad (7)$$

where a multiplier factor of 0.98 is used to take into account reduction in vapor pressure caused by a typical salinity of 34 psu.

140



3 Results and discussion

3.1 Simulated basic state of the winter NAO and SST

3.1.1 Space state

145 An empirical orthogonal function (EOF) analysis is performed on the normalized winter-averaged North Atlantic sea level pressure to obtain the first mode (EOF1) of the sea level pressure (SLP) field, that is, the NAO mode (Hurrell and Deser, 2009). Figure 1 shows the NAO modes of the observation and CMIP5-ESMs simulations. The NAO mode calculated with the observed SLP is significant, which explains 40.4% of the total variance. The explanation variances of the NAO mode by the models are close to those from the observations, ranged from 37.1% -53.4%. The result of
150 observation shows that the low-pressure action center of the NAO is at about 65 ° N and from 30 ° W to 20 ° E, and that the high-pressure action center is at 40 ° N and from 32 ° W to 20 ° E (Fig. 1). Compared with the location of the NAO action centers obtained with EOF1 of the same set of observed SLP from 1950 to 2010 by Jing et al. (2019), the location of the high-pressure action center is more eastward during 1902-2010, indicating that the location of the NAO action centers at different time periods will be slightly biased. This is consistent with previous results (Jung et al., 2003;
155 Moore et al., 2013; Jing et al., 2019). The simulated locations of the NAO action centers by the CMIP5-ESMs are basically reasonable, although there are some slight differences of the NAO action centers between different models and between the models and observation. Because the locations of the NAO action centers simulated by most of the CMIP5-ESMs in different NAO phases do not show the movements illustrated by the observation (the figure is



omitted), the differences between the models are not caused by the NAO period or the phase of the initial sign, but are
160 only related to the structures of models.

Figure 2 shows the observed and simulated multi-year average of winter SST in the NA (0-65°N). The
CMIP5-ESMs can basically reproduce low-temperature center near the Labrador Sea. The spatial correlation
coefficients with the observations are all above 0.98, reaching a significance level of 99%. Nevertheless, CMIP5-ESMs
underestimate the SST. Wang et al. (2014) pointed out that the underestimation of the multi-year mean SST in the NA
165 by the CMIP5-ESMs may be due to the weaker Atlantic meridional overturning circulation (AMOC) and the
unreasonable vertical structure of it (the weaker northward heat transport caused by shallower AMOC cell). In the term
of interannual variability of winter SST in the NA (0-65°N) (Fig. S1), all CMIP5-ESMs can reproduce the strong
interannual variability of SST in the Gulf Stream extension, but the simulated strong interannual variability of SST by
most models is more easterly than the observations. In addition, some models also simulate strong interannual
170 variability at higher latitudes that is not observed.

3.1.2 Temporal period

Figure 3a shows the periods of the NAO indexes calculated with the method proposed by Gong and Wang (2000)
based on the observation and with the method proposed by Zheng et al. (2013) based on the models. The significant
periods (at a 90% confidence level) of the observed NAO index are 2.3–2.7, 4.7–5.8, and 8.3 years, characterized by
175 interannual and decadal signals. The 13 CMIP5-ESMs can simulate significant interannual signals of the NAO, in



which most models can reproduce the interannual signals of 2 years and 4-6 years, while CanESM2, GFDL-ESM2G and IPSL-CM5A-LR can only reproduce the interannual signal of 2 years, and HadGEM2-CC / ES can only reproduce the interannual signal of 4-6 years. Compared with the observation, the model deviation of the NAO period is reflected on the decadal scale, which is consistent with the result of Wang et al. (2017) based on the annual NAO. Figure 3b shows the observed and simulated periods of winter area-averaged SST anomalies in the NA (0-65°N). The observed area-averaged SST anomalies have a significant interannual signal of 2-3 years. The 13 CMIP5-ESMs can reproduce the 2-4 year interannual signal of SST. Some models such as HadGEM2-ES, IPSL-CM5A-MR, IPSL-CM5B-LR and MRI-ESM1 can simulate the decadal signal of 8-20 years that is not observed, and some models even simulate the multi-decadal signal, such as CESM1-BGC, GFDL-ESM2M, HadGEM2-CC and NorESM1-ME.

Based on the above analysis, simulated periods of the NAO indexes and area-averaged SST anomalies on the decadal scale are different from the results of observations. In addition, the impact of the atmospheric anomalies (NAO) on SST in the NA is mainly reflected in the impact of local change of wind stress on the sea-air heat flux on the interannual scales (Eden and Jung, 2001; Chen et al., 2015; Han et al., 2016). Therefore, we will extract the interannual signal of 2-6 years by band-pass filter based on the periods of the NAO and area-averaged SST anomalies to evaluate the relationship between the simulated NAO and SST in the CMIP5-ESMs on the interannual scale.

3.2 Responses of NA (0-65°N) SST to the NAO

Figure 4 shows the regression coefficients (RCs) of the winter-averaged SST anomalies against the NAO indexes



on the interannual scale in the NA (0-65°N). The significant RCs between the observed NAO indexes and SST anomalies give out a tripole pattern along the meridional direction with positive RCs in the subtropical region (25-45°N) and negative RCs in the both tropical (0-25°N) and subpolar regions (45-65°N), which is consistent with Walter and Graf (2002) and Chen et al. (2015). Compared with the observation, only 7 models can reproduce the tripole pattern of the response of the SST to the NAO, and other 6 models, including CanESM2, HadGEM2-ES, IPSL-CM5A-MR, MPI-ESM-MR / LR and MRI- ESM1, generate unreasonably significant positive RCs in the subpolar region. In the subtropical region, all models produce weak positive RCs.

3.2.1 The role of wind speed

Since the influence of the NAO on the SST is mainly through the wind field in the NA (Zhou et al., 2006; Deser et al., 2010), in order to evaluate the mechanism of the influence of the simulated NAO on the SST in the NA (0-65°N), the response of the wind speed to the NAO should be firstly considered. Figure 5 shows the RCs of the sea surface wind speed anomalies against the NAO indexes on the interannual scale, which clearly shows a meridional tripole pattern with negative RCs in middle latitudes (30-40° N) and positive RCs in the both tropical and high latitudes (north of 40°N). This distribution pattern is closely similar to the NAO-SST relationship, which is consistent with the results of Cayan (1992), Marshall and Gareth (2003), Visbeck et al. (2003) and Deser et al. (2010). All the CMIP5-ESMs can reproduce the impact of the NAO on the sea surface wind field. During the positive phase of the NAO, wind speed is strengthened in the tropical NA and high latitudes, and weakened in middle latitudes. This is consistent with the fact



210 that during the positive phase of the NAO, the deepening of the low pressure in Iceland causes the abnormal east wind superimposed on the mid-latitude westerly wind, which weakens the mid-latitude wind speed (Deser et al., 2010; Chen et al., 2015).

According to the Eq. (3-6), the wind speed anomalies impact the SST by affecting the turbulent heat flux, but the wind speed only affects the magnitude of the turbulent heat flux. Therefore, when analyzing the effect of wind speed anomalies on the turbulent heat flux, it is necessary to consider the direction of the turbulent heat flux that is determined by the difference of temperature and specific humidity between the atmosphere and the sea surface. From the results of the multi-year averaged winter sensible / latent heat fluxes (SHF / LHF, Fig. S2), the observed and simulated SHF / LHF are all from the sea to the atmosphere. The main difference between the observations and models is that all models overestimate the SHF in the region north of 50° N, and some models such as CESM1-BGC, 220 GFDL-ESM2M / 2G, MPI- ESM1 and NorESM1-ME simulate the strong LHF in the subpolar NA that is not observed. Figure 6 shows the RCs of the SHF / LHF anomalies (positive values indicate the flux from the ocean to the atmosphere) against sea surface wind speed. The observed and simulated SHF / LHF anomalies in winter have a significant positive response to sea surface wind speed anomalies in the large area of the NA (0-65°N) except for the eastern region around 30 ° N on the interannual scale. Considering the directions of SHF / LHF, the increase in wind speed can significantly increase the turbulent heat flux transported from a large region of sea surface to the atmosphere. 225 Figure 7 shows the RCs of winter turbulent heat flux anomalies against the NAO indexes. The significant observed RCs between the NAO indexes and SHF / LHF anomalies in the NA (0-65°N) indicate a meridional tripole pattern



with negative RCs in the subtropical region and positive RCs in the both tropical and subpolar regions. The spatial distribution of the observed RCs is consistent with the results of Eden and Jung (2001) and Deser et al. (2010), and is generally consistent with the meridional distribution of the observed RCs of the sea surface wind speed anomalies against the NAO, indicating that the NAO-forced wind speed significantly impacts SHF / LHF. During the positive phase of the NAO, the increase of wind speed in the tropical and subpolar NA strengthens the turbulent heat flux transported from the ocean to the atmosphere, while the weakening of the wind speed in the subtropical NA weakens the turbulent heat flux. The CMIP5-ESMs can basically reproduce the significant RCs of turbulent heat flux anomalies against the NAO, for which the meridional distribution pattern is the same as the RCs of the wind speed anomalies against the NAO indexes. This demonstrates that simulated NAO-driven wind speed anomalies in winter also significantly impact the SHF / LHF.

3.2.2 The role of SHF

The variability of SHF and SST is related. According to the calculation formula of SST and SHF, the increase of SHF can decrease SST (Eq. 3-4), while the decreased SST can further decrease the SHF (Eq. 5). Therefore, when the variations of SST and SHF are negatively correlated, it can be inferred that the change of SHF influences SST, which means that the atmosphere forces the ocean; when the variations of SST and SHF are positively correlated, the change of SST leads to the change of SHF, which means that the ocean forces the atmosphere.

Figure 8a is the observation-based and simulated RCs of the winter-averaged SST anomalies to the



245 winter-averaged SHF anomalies. As expected, the anomalies of observed winter-averaged SST in the most regions of the NA show significant negative RCs against those of the observed SHF, which indicates that the atmospheric forces the North Atlantic Ocean in winter. Considering the significant relationship between the anomalies of SHF and those of wind speed / NAO indexes, it can be concluded that in winter the NAO can impact the SST by affecting the SHF in the most regions of the NA through the change of wind speed. There are 4 models which have positive RCs of

250 winter-averaged SST anomalies against the SHF anomalies in the most regions of the NA, namely HadGEM2-CC / ES and MPI-ESM-LR / MR, and almost all of models, except for NorESM1-ME, produce significant positive RCs in a large region of the subpolar NA. This can partly explain why the RCs of SST anomalies against the NAO in the subpolar NA in some models are inconsistent with the observation.

The positive RCs of the winter-averaged SST anomalies to the SHF anomalies simulated by models may be

255 induced by the unrealistic mechanism of air-sea interaction or other reasons that there may be other factors which play a dominant role to the variation of the SST and further impact the relationship between the SST anomalies and SHF anomalies. To investigate the reason of the positive relationship between the anomalies of SST and those of SHF simulated by most of models, lagged (leaded) covariance analysis of monthly anomalies of the SHF and SST is used and shown in Fig. 8b. The lagged or leaded time is two months. Here, the monthly SHF anomalies from October to

260 April and monthly SST anomalies from December to February of the same year are used. The observation-based and simulated covariance of SST and SHF anomalies both shows that the change of SHF is strongly related to change of SST in the subpolar and western subtropical NA. When the observed SST anomalies lag (lead) SHF anomalies by 2



months the covariance between the SHF and SST anomalies is negative (positive), which indicates a non-negligible impact of the SHF (SST) anomalies on the SST (SHF) anomalies in the subpolar and western subtropical NA. When
265 the change of SHF synchronizes with the change of SST, the covariance between the anomalies of the SHF and the SST is negative in the western subpolar and subtropical NA, which means that the forcing from the SHF to the SST is still dominated in the interaction between the SHF and SST, and the atmosphere forces the ocean through the SHF. As to the results of models, when the SST anomalies lags by 2 months onto SHF anomalies, all CMIP5-ESMs can reproduce the negative covariance between SHF and SST anomalies in the in most regions of subpolar and western
270 subtropical NA , but there are about half of these models simulate positive covariance in some regions of the subpolar NA, especially in GFDL-ESM2G and MRI-ESM1, indicating that other factors (such as the internal motion of ocean) have an impact on the variations of the SST in these regions beyond the SHF. When the change of SHF is synchronized with the change in SST, most models show that there is no effect of SHF on SST in the subpolar NA according to the positive covariance. This may be caused by faster feedback of the SST on atmospheric forcing in the models than that
275 in the observation, or the overestimated influence of other factors in those models.

3.2.3 The role of LHF

The LHF is calculated by wind speed and the difference between the saturation specific humidity of lower air and sea surface. Because the saturation specific humidity of sea surface is a function of SST (Eq. 7), according to the calculation formulas of SST and LHF (Eq. 3-4, 6-7), the relationship between LHF and SST is similar to the one



280 between SHF and SST. It means that when the variations of the SST and LHF are negatively correlated, the atmosphere forces the ocean through the LHF, and that when the variations of the SST and LHF are positively correlated, the ocean forces the atmosphere.

Figure 9a is the RCs of the observed and simulated winter-averaged SST anomalies against the LHF anomalies. The distributions of the RCs in the observation-based and modeled result are very similar to those of the SST anomalies against SHF anomalies. A main difference between these two sets of RCs is that the large range of negative values of the SST anomalies against LHF anomalies in the observation-based result and three models, namely CanESM2, CESM1-BGC, and NorESM1-ME, appear to be more southward than those of the SST anomalies against SHF anomalies. The simulated RCs of the SST anomalies against LHF anomalies are still positive in large regions of the subpolar NA in most of models, which can enhance the unrealistic response of the SST anomalies to the NAO in these regions.

285
290

Figure 9b shows the lagged (leaded) covariance between the anomalies of the LHF and SST. It can be seen that the change of the LHF is strongly related to the change of SST in most regions of the NA (0-65°N). When the observed SST anomalies lag (lead) those of the LHF by 2 months, there is an obviously negative (positive) covariance in a large region of NA, which indicates that the change of LHF (SST) can influence the change of SST (LHF) after two months. Compared with the relationship between the SHF anomalies and the lagged SST anomalies, the area where the LHF plays an impact on the lagged SST is larger, and covers most regions of the NA except for the western NA from 30°-40°N with positive RCs. When the changes of SST and LHF are synchronized, there is an obviously positive

295



300 covariance in the large region except in the subpolar NA, which is also different from the relationship of the
synchronized SHF anomalies and SST anomalies. This demonstrates that the time-scale of the LHF affecting SST is
shorter than that of the SHF affecting SST, and the ocean plays an important role in the interaction of LHF and SST.
The CMIP5-ESMs basically reproduce the lagged or leaded relationship between the SST anomalies and the LHF
anomalies, whereas the role of the ocean is overestimated. When the SST anomalies lag the LHF anomalies, most
models except for CESM1-BGC and NorESM1-ME simulate a large region of positive covariance in the subtropical
and subpolar NA, which only occurs in a small region in the observation-based results. When the two variables in the
305 models are synchronized, their positive covariance simulated by models is significantly stronger than that in the
observation-based results. It can be concluded that the oceanic forcing on the atmosphere through the LHF variation is
enhanced in the models, which results in a significant difference between the observed and simulated response of the
winter-averaged SST anomalies to the LHF anomalies (Fig. 9a).

3.2.4 The role of advection

310 The response of the SST anomalies to the NAO-driven SHF / LHF anomalies in the subtropical NA simulated by
CMIP5-ESMs can partly explain the unrealistic response of the SST anomalies to the NAO in some models, but cannot
explain this response in the other models that generate an incorrect response of the SST anomalies to the SHF / LHF
anomalies but a relatively reasonable response of the SST anomalies to the NAO. In the subtropical NA, it is also
worth noting that some models such as HadGEM2-CC / ES and MPI-ESM-LR / MR cannot reproduce the significant



315 negative RCs of the winter-averaged SST anomalies against the LHF anomalies that is observed in some areas of the subtropical NA (Fig. 9a), but these models can reproduce the RCs of the anomalies of winter-averaged SST against the NAO in these areas (Fig. 4). This suggests that there are other factors that are driven by the NAO, which may influence SST in the subtropical NA.

In addition to the turbulent heat flux, the changes of long / short wave radiation and the ocean circulation also
320 have effects on the change of SST. The long-wave radiation on the sea surface is mainly determined by SST, while the change of short-wave radiation does not have a strong relationship with NAO (the figure is omitted). The simulated relationship between SST and the NAO by the CMIP5-ESMs may be also related to the NAO-driven horizontal heat advection. Some studies have pointed out that during the positive phase of the NAO, the northeast advection is strengthened and the heat transfer from south to north is also enhanced. Compared with other seasons, this
325 phenomenon is more obvious in winter (Flatau et al., 2003; Bellucci et al., 2006). Nevertheless, some other studies have argued that the impact of ocean heat advection on the change of SST in the subtropical NA is mainly on the decadal scale (Delworth et al., 1998, Krahnmann et al., 2001). From the observation-based RCs of surface sea meridional velocity anomalies against the NAO in winter (Fig. 10), it can be seen that on the interannual scale, in the subtropical NA the observed meridional velocity (positive values indicate poleward advection) anomalies has a
330 significant positive response to the NAO, and in the subpolar NA it has a significant negative response to the NAO. According to the north-south gradient of SST, during the positive phase of the NAO, SST increases in the subtropical NA and decreases in the subpolar NA. It means that the NAO-driven northward heat transport anomalies based on



observation can have an impact on the response of the subtropical and subpolar SST anomalies to the NAO on the interannual scale. Except for the NorESM1-ME, all other CMIP5-ESMs can reproduce the significant positive RCs of the anomalies of the meridional velocity against the NAO in the subtropical NA, and all CMIP5-ESMs can reproduce the significant negative RCs of these two variables in the subpolar NA. In the subtropical NA, the impact of the NAO-driven advection-transport of the heat on the variation of the SST hides the modeled incorrect effect of the NAO-driven LHF on the SST anomalies, so that the SST anomalies show a positive response to the NAO in the subtropical NA, but the positive response is weaker relative to that in the observation. NorESM1-ME, which cannot reproduce the positive RCs of the meridional velocity anomalies to the NAO in the subtropical NA, can correctly reproduce the response of the SST anomalies to the LHF anomalies, and thus also reproduce the positive response of the SST anomalies to the NAO in the subtropical NA. In the subpolar NA, the response of the heat meridional transport to the NAO also can explain partly that some models (such as GFDL-ESM2G / 2M) can reproduce a reasonable response of the SST anomalies to the NAO with an unrealistic response of the SST anomalies to the NAO-driven turbulent heat flux.

4 Conclusion

We evaluated the influence mechanism of the NAO on the SST in the NA (0-65°N) simulated by CMIP5-ESMs. Because there is a deviation between the simulated and observed periods of the NAO indexes / area-averaged SST on the decadal scale, we mainly evaluated the simulation of the relationship between the winter-averaged SST and NAO



350 by 13 CMIP5-ESMs on the interannual scale.

Based on the observations, the response of winter-averaged SST anomalies to the NAO shows a significant tripolar distribution along the meridian in the NA. Only 7 models can reproduce an observed tripolar pattern of the response of SST anomalies to the NAO, and other 6 models produce a significant positive response of the SST anomalies to the NAO that is not observed in some areas of the subpolar NA (45-65°N). In the subtropical NA
355 (25-45°N), all models simulate weaker positive responses of SST anomalies to the NAO.

Further evaluation of the response mechanism of the winter-averaged SST anomalies to the NAO simulated by the 13 CMIP5-ESMs in the NA shows that the models can basically reproduce the impact of winter NAO-driven wind speed anomalies on turbulent heat flux anomalies in the NA, but the relationship between the anomalies of the turbulent heat flux and SST simulated by most of models is inconsistent with the observation-based results. In the
360 subpolar NA, the variability of SHF and LHF can impact the variations of the SST in the observation-based results, whereas the relationship between the anomalies of the turbulent heat flux and SST is contrary in most of the models, leading to the unreasonable positive response of the SST anomalies to the NAO in some models. The similar phenomenon also occurs in a large area of the subtropical NA where the variability of LHF and SST is mainly related. Different from the observation, there is unreasonable positive response of the SST anomalies to the LHF anomalies
365 because the role of the ocean in the air-sea interaction is overestimated. Besides the heat turbulent flux, there are other factors that can affect the relationship of the SST and NAO. The observed meridional velocity anomalies have a significant positive response to the NAO, which can be reproduced by most of the models, so the increase of meridional



370 heat transport leads to the increase of SST in the subtropical NA and the decrease of meridional heat transport leads to
the decrease of SST in the subpolar NA during the positive phase of the NAO. This mechanism probably conceals the
unreasonable impact of the heat turbulent flux anomalies on the SST anomalies in some models, so that the simulated
375 response of the SST anomalies to the NAO by all models is positive in the subtropical NA, which is also reflected in
the observation-based results, although the response intensity in the models is much weaker than that in the
observation-based results.

375 Data availability.

The addresses of downloading all data used in this study have been described in Sect. 2.1. All data for results are
available by contacting the corresponding author.

Author contributions.

YJJ, YCL and YFX designed the research. YJJ analyzed the data under the guidance of YCL and YFX, and prepared
380 the manuscript with contributions from YCL and YFX.

Competing interests.

The authors declare that they have no conflict of interest.

Acknowledgements.

All the authors thank the European Centre for Medium Range Weather Forecasts (ECMWF) for providing the sea level
385 pressure data, the Hadley Centre Global Sea Ice and Sea Surface Temperature (HadiSST) for providing sea surface



temperature data, and National Oceanic and the Atmospheric Administration (NOAA) for providing the 10-m wind speed, turbulent heat flux and sea water meridional velocity data. The authors also thank those institutions that developed the CMIP5 Earth System Models and provided simulation results.

Financial support.

390 This work was supported jointly by the National Key Research and Development Program of China (No. 2016YFB0200800) and the National Natural Science Foundation of China (Grant No. 41530426).



References

- 395 Bellucci, A., and Richards, K. J.: Effects of NAO variability on the North Atlantic Ocean circulation, *Geophys. Res. Lett.*, 33(2), L02612, <https://doi.org/10.1029/2005gl024890>, 2006.
- Behringer, D. W., and Xue, Y.: Evaluation of the global ocean data assimilation system at NCEP: The Pacific Ocean. Proc. Eighth Symp. on integrated observing and assimilation systems for atmosphere, oceans, and land surface, Seattle, WA, Amer. Meteor. Soc., 2.3, https://ams.confex.com/ams/84Annual/techprogram/paper_70720.htm, 2004. Cayan, D. R.: Latent and sensible heat flux anomalies over the northern oceans: driving the sea surface temperature, *J. Phys. Oceanogr.*, 22, 859–881, [https://doi.org/10.1175/1520-0485\(1992\)0222.0.CO;2](https://doi.org/10.1175/1520-0485(1992)0222.0.CO;2), 1992.
- 400 Chen, H., Schneider, E. K., and Wu, Z.: Mechanisms of internally generated decadal-to-multidecadal variability of SST in the Atlantic Ocean in a coupled GCM, *Clim. Dyn.*, 46(5), 1-30, <https://doi.org/10.1007/s00382-015-2660-8>, 2015.
- 405 Compo, G.P., Whitaker, J.S., Sardeshmukh, P.D., Matsui, N., Allan, R.J., Yin, X., Gleason, B.E., Vose, R.S., Rutledge, G., Bessemoulin, P., Brönnimann, S., Brunet, M., Crouthamel, R.I., Grant, A.N., Groisman, P.Y., Jones, P.D., Kruk, M., Kruger, A.C., Marshall, G.J., Mauerer, M., Mok, H.Y., Nordli, Ø., Ross, T.F., Trigo, R.M., Wang, X.L., Woodruff, S.D., and Worley, S.J.: The Twentieth Century Reanalysis Project, *Quarterly J. Roy. Meteorol. Soc.*, 137, 1-28, <http://dx.doi.org/10.1002/qj.776>, 2011.
- 410 Czaja, A., and Frankignoul, C.: Observed impact of Atlantic SST anomalies on the North Atlantic oscillation, *J.*



Clim., 15, 606– 623, <https://doi.org/10.1175/1520-0442>, 2002.

Delworth, T. L., and Mehta, V. M.: Simulated interannual to decadal variability in the tropical and sub-tropical North Atlantic. *Geophys. Res. Lett.*, 25(15), 2825-2828, <https://doi.org/10.1029/98gl02188>, 1998.

Deser, C., Alexander, M. A., Xie, S. P., et al.: Sea surface temperature variability: patterns and mechanisms, *Annu. Rev. Mar. Sci.*, 2(1), 115-143, <https://doi.org/10.1146/annurev-marine-120408-151453>, 2010.

Eden, C., and Jung, T.: North Atlantic interdecadal variability: oceanic response to the North Atlantic Oscillation (1865-1997), *J. Clim.*, 14(5), 676-691, [https://doi.org/10.1175/1520-0442\(2001\)0142.0.CO;2](https://doi.org/10.1175/1520-0442(2001)0142.0.CO;2), 2001.

Flatau, M. K., Talley, L., and Niiler, P. P.: The North Atlantic Oscillation, surface current velocities, and SST changes in the subpolar North Atlantic, *J. Clim.*, 2355-2369, <https://doi.org/10.1175/2787.1>, 2003.

Gastineau, G., D'Andrea, F., Frankignoul, C.: Atmospheric response to the North Atlantic Ocean variability on seasonal to decadal time scales. *Clim. Dyn.* 40(9-10), 2311-2330. <https://doi.org/10.1007/s00382-012-1333-0>. 2012.

Gong, D. Y., and Wang, S. W.: The North Atlantic Oscillation index and its interdecadal variability, *Chinese J. Atmos. Sci.*, 24, 187–192, <https://doi.org/10.3878/j.issn.1006-9895.2000.02.07>, 2000.

Han, Z., Luo, F. F., and Wan, J. H.: The observational influence of the North Atlantic SST tripole on the early spring atmospheric circulation, *Geophys. Res. Lett.*, 43, 2998–3003, <https://doi.org/10.1002/2016GL068099>, 2016.

Hurrell, J. W., and Deser C.: North Atlantic climate variability: the role of the North Atlantic Oscillation, *J. Marine Syst.*, 79(3), 231-244, <https://doi.org/10.1016/j.jmarsys.2009.11.002>, 2009.



- Jing, Y., Li, Y. C., Xu, Y. F., and Fan, G. Z.: Influences of different definitions of the winter NAO index on NAO action centers and its relationship with SST, *Atmos. Oceanic Sci. Lett.*, 12(5), 320-328, <https://doi.org/10.1080/16742834.2019.1628607>, 2019.
- Jung, T., Hilmer, M., Ruprecht, E., Kleppek, S., Gulev, S.K., and Zolina, O.: Characteristics of the recent eastward shift of interannual NAO variability, *J. Clim.*, 16(20), 3371-3382, [https://doi.org/10.1175/1520-0442\(2003\)016<3371:cotres>2.0.co;2](https://doi.org/10.1175/1520-0442(2003)016<3371:cotres>2.0.co;2), 2003.
- Krahmann, G., Vsbeck, M., and Reverdin, G.: Formation and propagation of temperature anomalies along the North Atlantic Current, *J. Phys. Oceanogr.*, 31(5), 1287-1303, [https://doi.org/10.1175/1520-0485\(2001\)0312.0.CO;2](https://doi.org/10.1175/1520-0485(2001)0312.0.CO;2), 2001.
- Liu, H. L., Wang, C. Z., Lee, S. K. and Enfield, D.: Atlantic warm pool variability in the CMIP5 Simulations, *J. Clim.*, 26, 5315-5336, <https://doi.org/10.1175/JCLI-D-12-00556.1>, 2013.
- Marshall, and Gareth, J.: Trends in the Southern Annular Mode from observations and reanalyses, *J. Clim.*, 16, 4134–4143, [https://doi.org/10.1175/1520-0442\(2003\)016<4134:TITSAM>2.0.CO;2](https://doi.org/10.1175/1520-0442(2003)016<4134:TITSAM>2.0.CO;2), 2003.
- Moore, G. W. K., Renfrew, I. A., and Pickart, R. S.: Multidecadal mobility of the North Atlantic Oscillation, *J. Clim.*, 26(8), 2453-2466, <https://doi.org/10.1175/jcli-d-12-00023.1>, 2013.
- Rayner, N. A., Parker, D. E., Horton, E. B., Folland, C. K., Alexander, L. V., Rowell, D. P., Kent, E. C., and Kaplan, A.: Global analyses of sea surface temperature, sea ice, and night marine air temperature since the late nineteenth century, *J. Geophys. Res.*, 108, 4407, <https://doi.org/10.1029/2002JD002670>, 2003.



- Rivière, G., and Orlanski, I.: Characteristics of the Atlantic storm-track eddy activity and its relation with the North Atlantic Oscillation, *J. Atmos. Sci.*, 64(2), 241-266, <https://doi.org/10.1175/jas3850.1>, 2007.
- Stoner, A. M. K., Hayhoe, K., and Wuebbles, D. J.: Assessing general circulation model simulations of atmospheric teleconnection patterns, *J. Clim.*, 22, 4348-4372, <https://doi.org/10.1175/2009JCLI2577.1>, 2009.
- 450 Sun, C., Li, J. P., and Jin, F. F.: A delayed oscillator model for the quasi-periodic multidecadal variability of the NAO, *Clim. Dyn.*, 45(7), 2083-2099, <https://doi.org/10.1146/10.1007/s00382-014-2459-z>, 2015.
- Sutton, R., and Mathieu, P. P.: Response of the atmosphere–ocean mixed-layer system to anomalous ocean heat-flux convergence, *Q. J. Roy. Meteor. Soc.*, 128(582), 1259-1275, <https://doi.org/10.1256/003590002320373283>, 2002.
- 455 Taylor, K. E., Stouffer, R. J., and Meehl, G. A.: An overview of CMIP5 and the experiment design, *Bull. Amer. Meteor. Soc.*, 93, 485–498, <https://doi.org/10.1175/BAMS-D-11-00094.1>, 2012
- Trigo, R. M., Osborn, T. J., and Corte-Real, J. M.: The North Atlantic Oscillation influence on Europe: climate impacts and associated physical mechanisms, *Clim. Res.*, 20, 9–17, https://doi.org/10.3354/cr020_009, 2002.
- Visbeck, M., Chassignet, E. P., Curry, R. G., Delworth, T. L., Dickson, R. R., and Krahnmann, K.: The ocean’s response to North Atlantic Oscillation variability, American Geophysical Union, USA, <https://doi.org/10.1029/134GM06>, 2003.
- 460 Walker, G.T.: Correlation in seasonal variations of weather-A further study of world weather, *Mon. Wea. Rev.*, 53, 252–254, [https://doi.org/10.1175/1520-0493\(1925\)53<252:CISVOW>2.0.CO;2](https://doi.org/10.1175/1520-0493(1925)53<252:CISVOW>2.0.CO;2), 1924.
- Walter, K., and Graf, H. F.: On the changing nature of the regional connection between the North Atlantic Oscillation

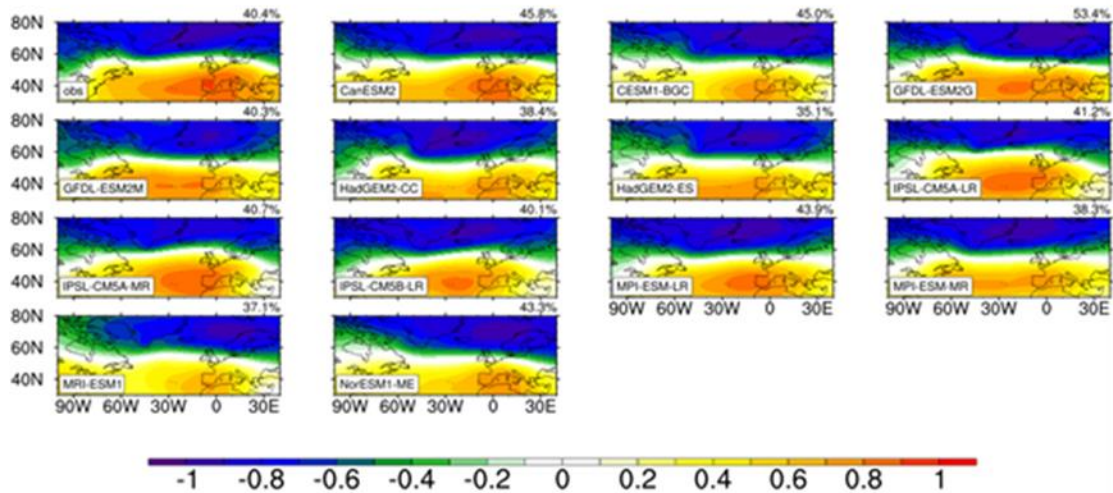


- 465 and sea surface temperature, *J. Geophys. Res.*, 107, 7-13, <https://doi.org/10.1029/2001jd000850>. 2002.
- Wang, C. Z, Zhang, L. P, Lee, S. K., Wu, L. X, and Mechoso, C. R.: A global perspective on CMIP5 climate model
biase, *Nat. Clim. Change*, 4(3), 201-205, <https://doi.org/10.1038/nclimate2118>. 2014.
- Wang, X. F., Li, J. P., Sun, C., and Liu T.: NAO and its relationship with the Northern Hemisphere mean surface
temperature in CMIP5 simulations, *J. Geophys. Res. Atmos.*, 122, <https://doi.org/10.1002/2016JD025979>, 2017.
- 470 Wen, N., Liu, Z. Y., Liu, Q. Y., Frankignoul, C.: Observations of SST, heat flux and North Atlantic Ocean-atmosphere
interaction, *Geophys. Res. Lett.*, 322(24), 348-362, <https://doi.org/10.1029/2005GL024871>, 2005.
- Woollings, T., Franzke, C., Hodson, D. L. R., Dong, B., Barnes, E. A., Raible C. C., and Pinto, J. G.: Contrasting
interannual and multidecadal NAO variability, *Clim. Dyn.*, 45, 539–556,
<https://doi.org/10.1007/s00382-014-2237-y>, 2014.
- 475 Yulaeva, E., Schneider, N., Pierce D., and Barnett T.: Modeling of North Pacific climate variability forced by oceanic
heat flux anomalies, *J. Clim.*, 14, 4027–4046, [https://doi.org/10.1175/1520-0442\(2001\)0142.0.CO;2](https://doi.org/10.1175/1520-0442(2001)0142.0.CO;2), 2001.
- Zheng, F., Li, J. P., Clark R. T., and Nnamchi, H. C., Simulation and projection of the Southern Hemisphere annular
mode in CMIP5 models, *J. Clim.*, 26(24), 9860–9879, <https://doi.org/10.1007/10.1175/JCLI-D-13-00204.1>, 2013.
- Zhou, T. J., Yu, R., Gao, Y., Helge, D.: Ocean-atmosphere coupled model simulation of North Atlantic interannual
480 variability I: Local air-sea interaction, *Acta Meteorol. Sin.*, 2006.

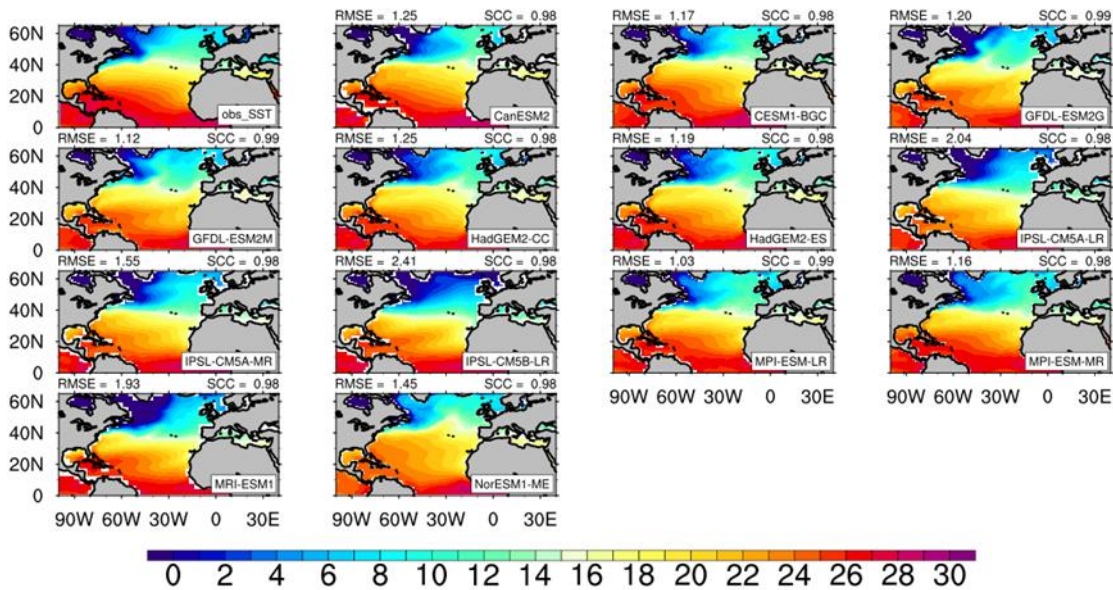


Table 1. CMIP5 models used in this study.

models	Sponsor, Country	Ocean	Marine Resolution
		Model	(lat×lon)
CanESM2	Canada, CCCMA	CanOM4	0.98° × 1.4°
CESM1-BGC	U.S.A, NSF-DOE-NCAR	POP2	320 × 384 grid points (gx1v3)
GFDL-ESM2G	U.S.A, NOAA-GFDL	GOLD	0.6° × 1.0° (tripolar)
GFDL-ESM2M	U.S.A, NOAA-GFDL	MOM4.1	0.6° × 1.0° (tripolar)
HadGEM2-CC	Britain, MOHC	HadGOM2	0.3°–1° × 1°
HadGEM2-ES	Britain, MOHC	HadGOM2	0.3°–1° × 1°
IPSL-CM5A-LR	France, ISPL	ORCA2	2° × 2°
IPSL-CM5A-MR	France, ISPL	ORCA2	2° × 2°
IPSL-CM5B-LR	France, ISPL	ORCA2	2° × 2°
MPI-ESM-LR	Germany, MPI-M	MPI-OM	1.5° × 1.5°
MPI-ESM-MR	Germany, MPI-M	MPI-OM	0.4° × 0.4°
MRI-ESM1	Japan, MRI	MRI-COM3	0.5° × 1°
NorESM1-ME	Norway, NCC	MICOM	0.5° × 1°



485 Figure 1 EOF1 of observed and simulated normalized winter-averaged sea level pressure over the particular region of the North Atlantic (30 -80°N; 100°W-40°E). The time periods for the observation and models range from 1902 to 2010 and 1897 to 2005, respectively.



490 Figure 2 The observed and simulated winter-averaged multi-year mean SST (°C) in the North Atlantic (NA) (0-65°N). The time periods for the observation and models range from 1902 to 2010 and 1897 to 2005, respectively. SCCs is the spatial correlation coefficient of SST between model and observation, and RMSE is the root-mean-square error.

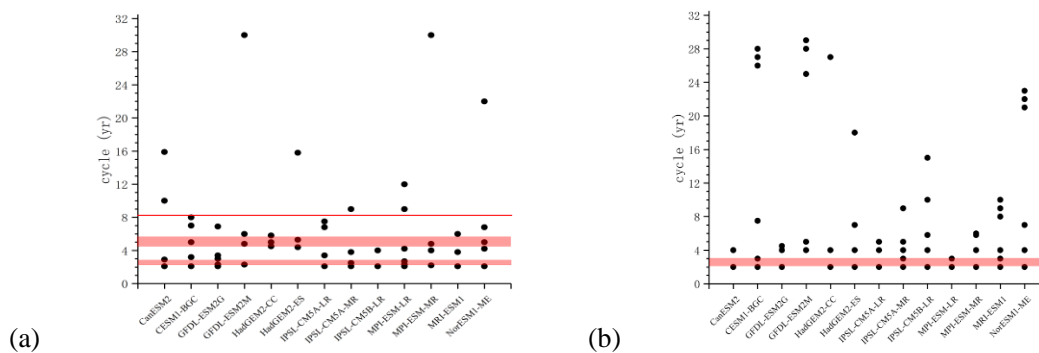
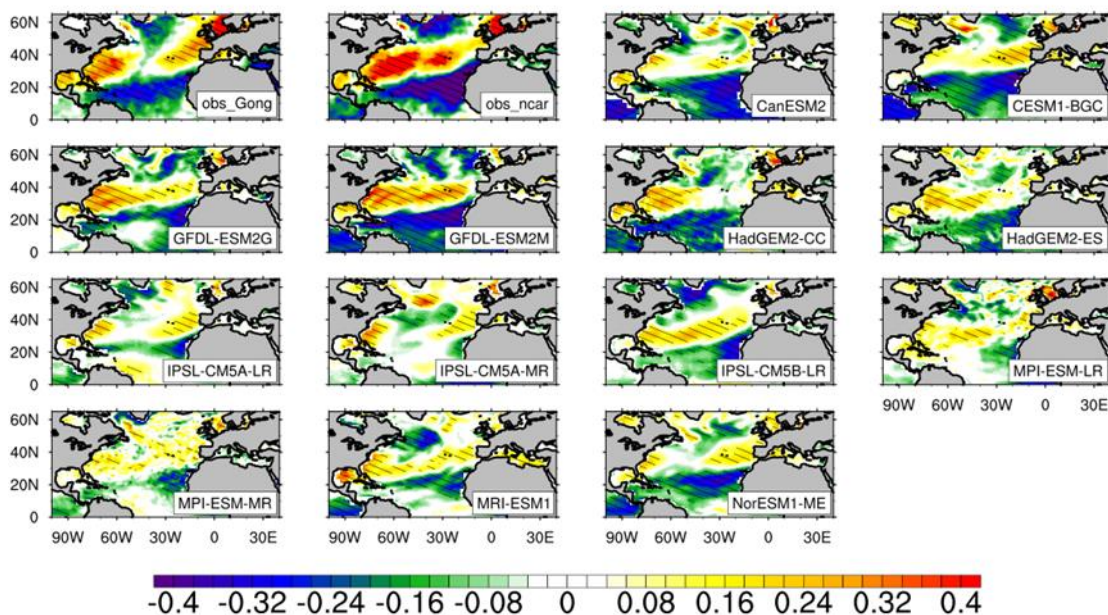


Figure 3 Periodicities of the observed and simulated winter-averaged NAO indexes (a) and area-averaged SST anomalies (b) in the NA (0-65°N), determined by power spectrum analysis. The periodicities are determined by calculating the red noise confidence interval and choosing those at the 90% confidence level. The time periods for the observation and models range from 1902 to 2010 and 1897 to 2005, respectively.

495

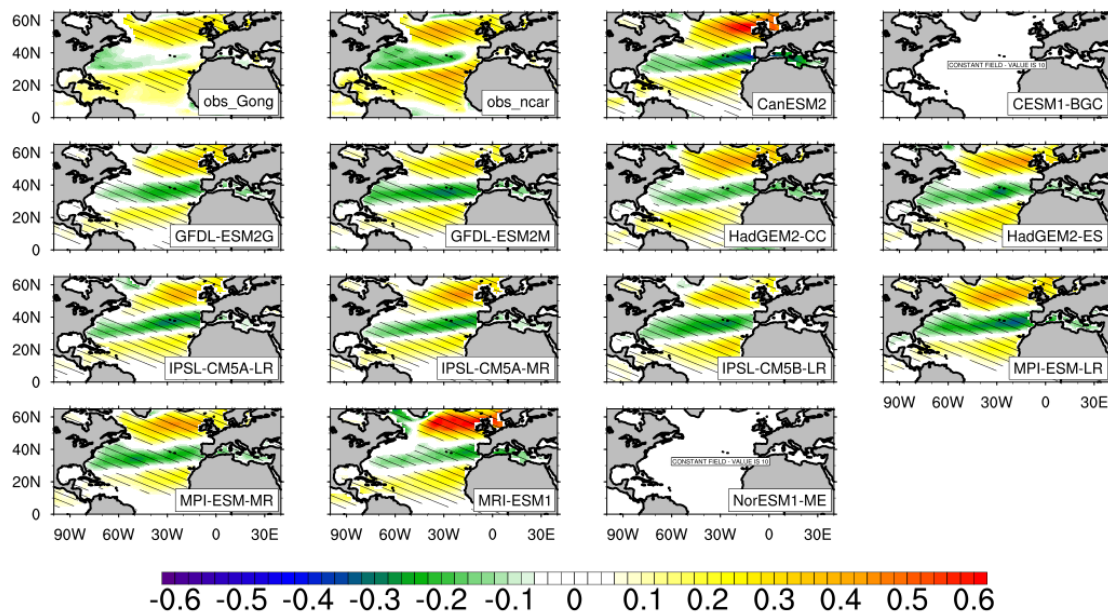


500

Figure 4 The observed and simulated regression coefficients (RCs) of the winter-averaged SST anomalies against the NAO indexes on the interannual scale. Shaded areas indicate that RCs are statistically significant at the 95% confidence level of the Student's t-test. The obs_Gong is the RCs of observed SST to the NAO indexes based on Gong



method, and obs_ncar is the RCs of observed SST to the NAO indexes provided by NCAR. The time periods for the observation and models range from 1902 to 2010 and 1897 to 2005, respectively.



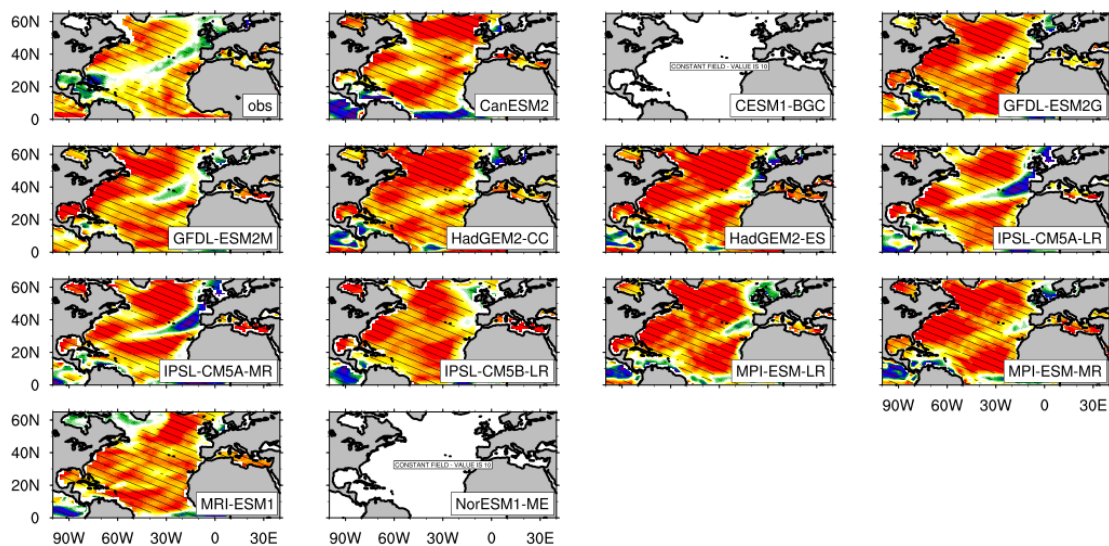
505

Figure 5 Same as FIG.4 but for the winter-averaged sea surface wind speed anomalies against the NAO indexes. A missing panel means the model output is not available.

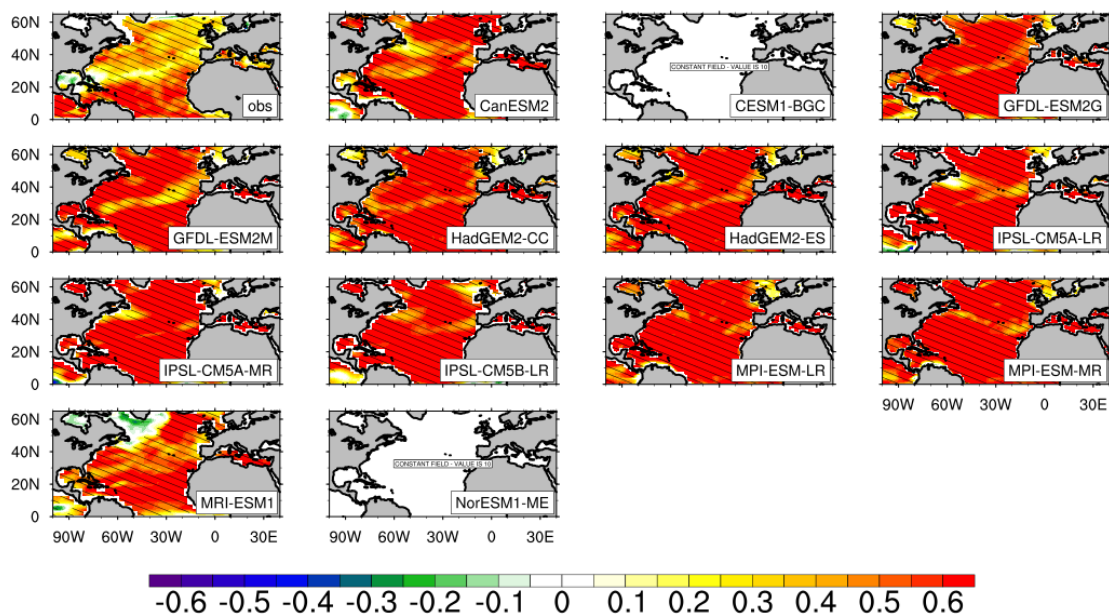
510



(a)



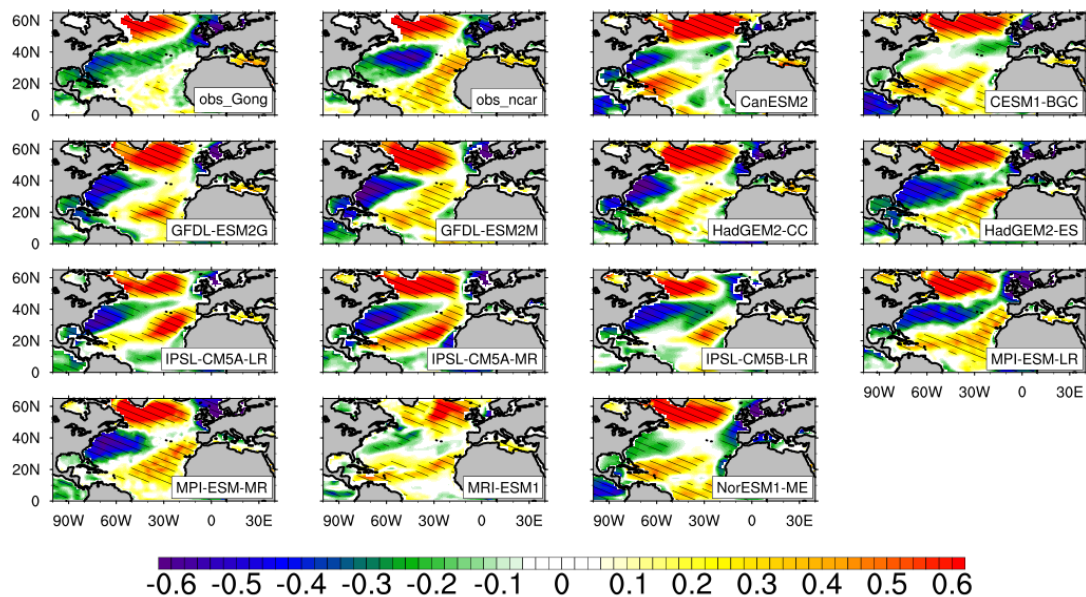
(b)



515 Figure 6 Same as FIG. 4 but for the winter-averaged sensible heat flux (SHF, a) / latent heat flux (LHF, b) anomalies against the sea surface wind speed anomalies. The positive values of the SHF / LHF indicate flux from the ocean to the atmosphere. A missing panel means the model output is not available.



(a)



520

(b)

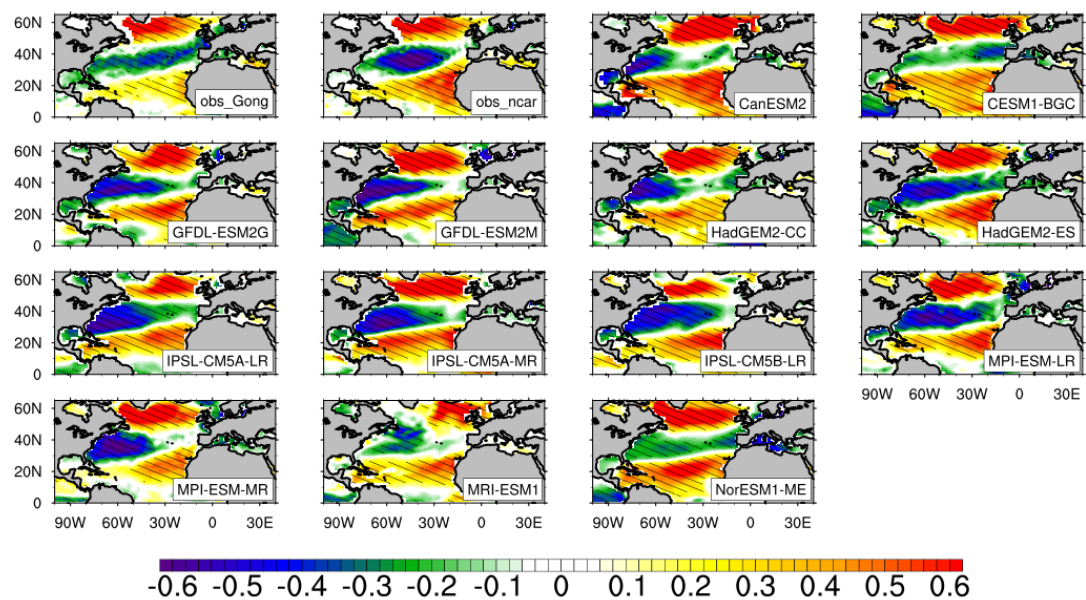
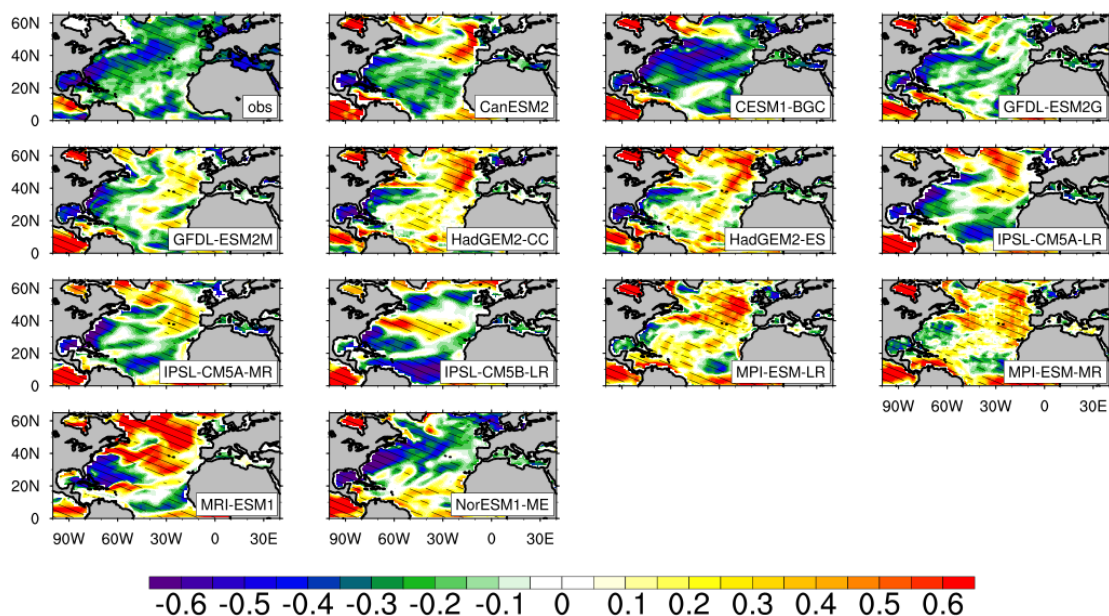


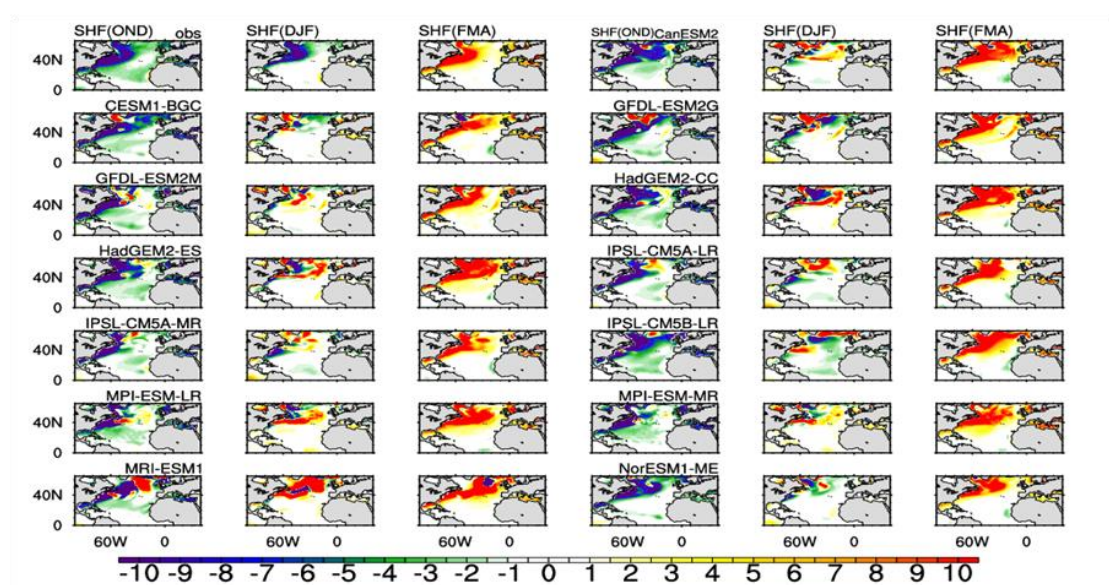
Figure 7 Same as FIG. 6 but for against the NAO indexes.



525 (a)



(b)



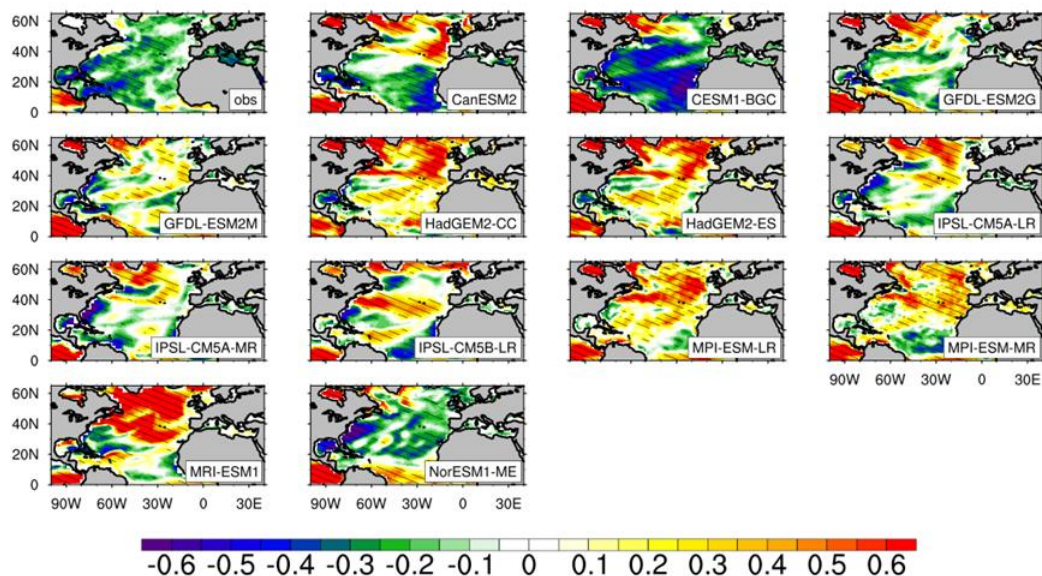
530

Figure 8 (a) Same as FIG. 4 but for the winter-averaged SST anomalies against the SHF anomalies. (b) The lagged (leaded) covariance between monthly SHF anomalies from October to December / from February to April with the



SST anomalies from December to January. OND refers to the SHF from October to December, and FMA refers to the SHF from February to April.

(a)



535 (b)

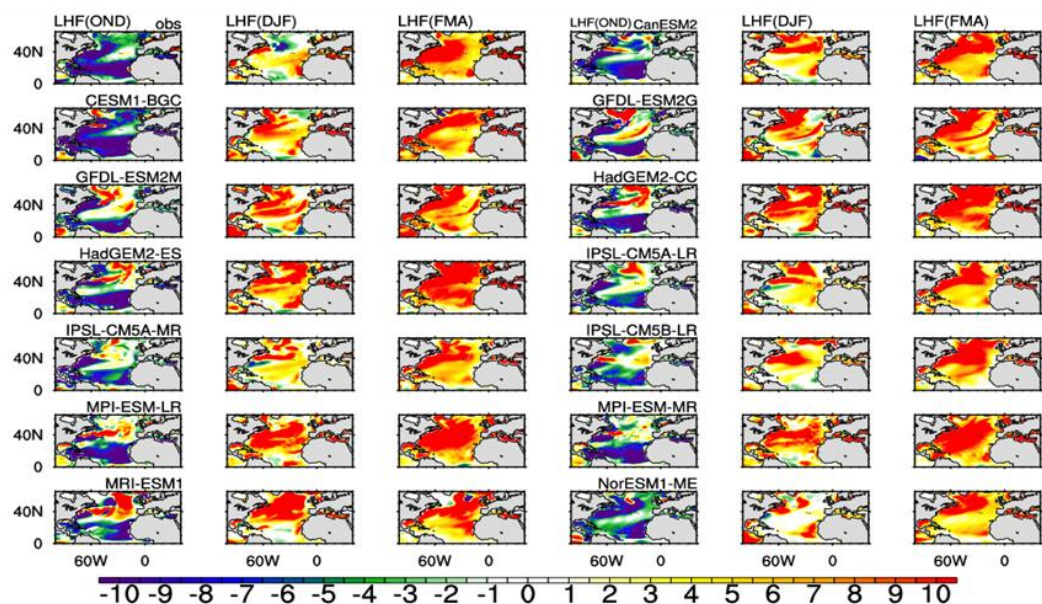
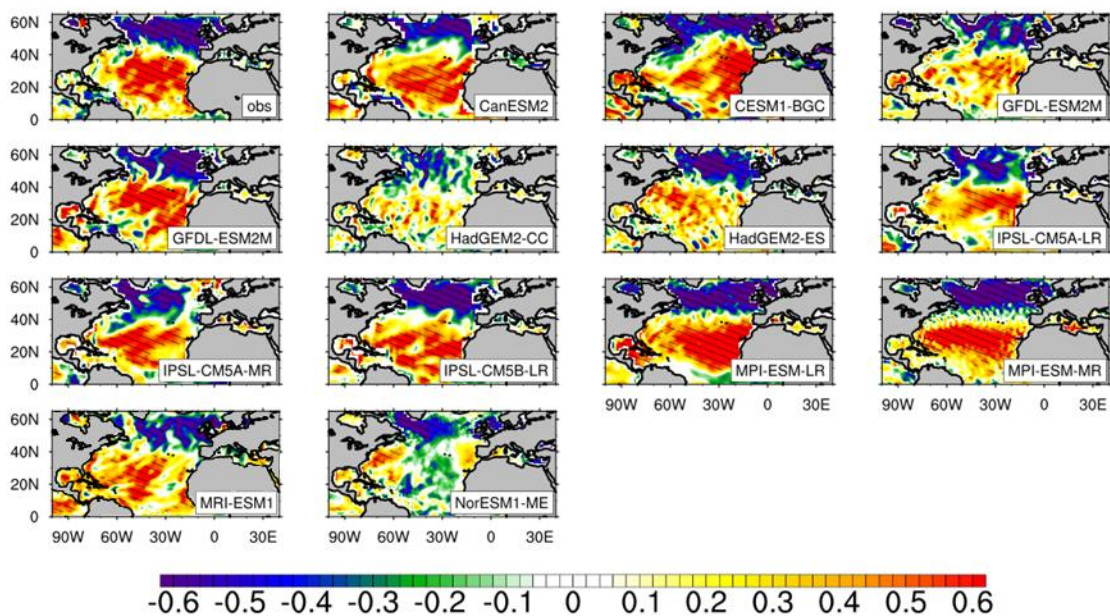


Figure 9 Same as FIG. 8 but for the LHF.



540 Figure 10 Same as FIG.4 but for the winter-averaged sea surface meridional velocity anomalies against the NAO index provided by NCAR.